Finite element analysis of vehicle-structure interactions during launching of remotely piloted air-vehicles

C S Manohar
S Venkatesha

Department of Civil Engineering
Indian Institute of Science
Bangalore 560 012

S Sadasivan

Aeronautical Development Establishment
C V Raman Nagar, Bangalore 560 093

Abstract

The problem of finite element modeling and analysis of dynamic interactions between the launcher and a remotely piloted aircraft structure is considered. The governing equations of motion are shown to constitute a set of ordinary differential equations with time varying structural matrices. An iterative strategy that treats separately the dynamics of the launcher and the aircraft is developed. The strategy is shown to be capable of including the effects of several other sources of dynamic excitations such as guideway unevenness, rocket thrust, running motor, and transients during the initial release and final take-off of the aircraft. The usefulness of the analysis in delineating the relative importance of contributions from various sources of excitations is demonstrated.

1.0 Background

The problem of dynamic interactions between moving vehicles and bridge structures has been widely studied in the existing literature: see for example the book by Fryba (1999) which extensively documents classical treatment of problems involving beams, plates and elastic half spaces. In structural engineering context, these problems are widely encountered in the study of bridge-vehicle interactions (Fryba 1996, Kirekegaard *et al.*, 1997). These problems also occur in other branches of engineering such as in the study of remotely piloted air-vehicles (RPVs) during launching, roller coasters, elevated guideways and high speed machining. In these problems the nature of travelling load and the dynamical properties of the moving vehicle and the supporting structure relative to each other, are quire different from what is generally encountered in bridge engineering field. There could be fundamental differences in the problem perception as well. This is true, for example, in the case of unmanned aircraft and launcher systems, wherein, the vibration levels inside the aircraft, during the launch phase, need to be reasonably estimated so that the mountings of the various equipment, that these vehicles carry, are adequately designed and qualified for. Similarly, in modern machining problems, the moving heads do not travel at constant velocities but with a programmed servo/feedback controlled motion profiles. This motion produces interaction forces between the moving

parts and the supporting structures that are broad banded and much different from those encountered in bridge engineering. In the context of elevated guideways, questions on passenger ride quality and minimization of airborne noise radiating from the elevated guideways are relevant. Thus the increase in the sophistication of the technologies involved calls for increased ability to predict the structural responses accurately. This requirement has spurred the development of sophisticated computational tools to model and analyze the problem of vehicle-structure interaction problems (see, for example, Ting *et al.*, 1975, Filho 1978, Genin and Ting 1979, Lin and Trethewey 1990, Green and Cebon 1996 and Yang and Fonder 1996).

There are several complicating features associated with the study of vehicle-structure interactions: some of these are as follows:

- The inclusion of vehicle flexibility/inertia makes the governing equations of motion to possess time varying coefficients, which, in turn, lead to time dependent structural matrices when the equations are spatially discretized.
- The motion of the vehicle on the vibrating profile of the supporting structure leads to Coriolis terms in equations of motion.
- While in transit, the vehicle may lose and regain contact with the supporting structure, thereby, making the problem highly nonlinear in nature.
- Structural imperfections, such as, guide way unevenness and non-circularity of wheels, have significant effect on the dynamic interactions, especially, for higher speeds of vehicle motion. These imperfections may evolve in time due to excursions of the stresses beyond the yield limits during each duty cycle of operation.
- The motion of vehicle is characterized by several influencing parameters such as direction of motion, velocity, acceleration/braking, path of travel, presence of vibrating systems in the moving vehicle.

2.0 Present study

In the present study we consider the problem of dynamic interactions between a RPV and the launcher during the launch phase. Figures 1 and 2 show the RPV resting on the launcher in its ready to launch position. Here the RPV, with its engine running, rests on a shuttle with twelve wheels that are designed to travel on a set of six rails fitted to the launcher. Before launching, the RPV and the shuttle system are held in position with the help of a shear pin. The launching is triggered by firing of a set of rockets housed inside the shuttle. The thrust developed by the rockets overcomes the strength of the shear pin, which sets the shuttle-RPV system into motion. When the shuttle reaches the end of the launcher, its motion is arrested by a visco-elastic braking system. At this stage, the RPV gets released from the shuttle and it gets airborne with a specified exit velocity. During the time period between the firing of the rockets and the RPV exiting the launcher, the RPV-launcher system would be subjected to intense dynamic environment. Figure 3 shows typical plots of acceleration time histories acquired during field studies. The first of these records apparently shows instrument saturation. The launching here is initiated at about 0.6 second and the aircraft gets airborne by about 1.3 seconds. The severity of the observed vibrations was a cause for concern on the integrity of various components in the RPV. A study of these figures, at the outset, does not enable one to delineate the various

contributing factors to the observed trend in vibration time histories. If these vibrations are to be mitigated one needs to understand, at least qualitatively, the various mechanisms that come into play in producing these vibration time histories. The objective of the present study is to construct a suitable mathematical model, which should enable to estimate the effects of various sources of dynamic excitations on the RPV response. Specifically, we are interested in estimating the vibration levels at the sensitive points on the RPV where surveillance equipment would be mounted. The sources of dynamic excitations here are the forces due to RPV motion, running engine in the RPV, track unevenness, rocket thrust/blast, transients due to shear pin break, visco-elastic braking and the vehicle release from the shuttle. The mathematical model for the system is made using finite element (FE) modeling using a commercial FE software (NISA).

3.0 FE modeling and iterative solution strategy

With a view to illustrate the nature of structural matrices that would arise in modeling of VSI problems, we consider an idealization of VSI problems consisting of an Euler-Bernoulli beam and a moving oscillator system (figure 4). The beam has a span of *L*, flexural rigidity of *EI*, mass per unit length *m* and is taken to be viscously damped. The oscillator has a sprung mass m_1 and unsprung mass m_2 and is taken to travel with a velocity *v* and acceleration *a*. Denoting respectively by *M, C* and *K*, the structure mass, damping and stiffness matrices for the beam, the governing equation of motion for the beam-moving oscillator system, obtained using FE discretization, can be shown to be of the form (Filho 1978)

$$\begin{bmatrix} [M]+[m]^* & \{0\} \\ \{0\} & m_1 \end{bmatrix} \begin{Bmatrix} \ddot{d} \\ \ddot{w} \end{Bmatrix} + \begin{bmatrix} [C]+[c]^* & -c[N]^T \\ -c[N]^T & c \end{bmatrix} \begin{Bmatrix} \dot{d} \\ \dot{w} \end{Bmatrix} + \begin{bmatrix} [K]+[k]^* & -k[N]^T \\ -c\dot{x}[N]_x - k[N] & k \end{bmatrix} \begin{Bmatrix} d \\ w \end{Bmatrix} = \begin{Bmatrix} [N]^T(m_1+m_2)g \\ 0 \end{Bmatrix} \quad \text{.....(1)}$$

Here *g*= acceleration due to gravity, *d(t)*= beam degrees of freedom, *[N]*= beam shape functions, the superscript T denotes matrix transpose and

$$[m]^* = m_2[N]^T[N]$$

$$[c]^* = 2m_2\dot{x}[N]^T[N]_x + c[N]^T[N]$$

$$[k]^* = m_2\dot{x}^2[N]^T[N]_{xx} + m_2\ddot{x}[N]^T[N]_x + k[N]^T[N]_x \quad \text{.....(2)}$$

These equations are valid for the time interval during which the oscillator is on the beam with *t=0* being the time instant at which the oscillator enters the beam. In these equations, $[.]_x$ and $[.]_{xx}$ denotes, respectively, the derivatives with respect to spatial co-ordinate *x*. Furthermore it should be noted that $x(t)=vt+0.5at^2$. It is important to note that the structural matrices in the above equations are asymmetric and time varying in nature and, consequently, one has to use direct integration methods to obtain the responses.

When the supporting structure and the vehicle model are more complex, as in the case of the RPV-launcher system shown in figures 1 and 2, it becomes necessary to adopt elaborate FE models for both the vehicle and the supporting structure. In such a case,

setting up equations of motion, as in equation 1, although possible in principle, becomes unwieldy unless one develops special purpose softwares to deal with this situation. To the best of authors' knowledge, commercially available FE softwares do not have capabilities to deal with this type of problems. Consequently, it becomes necessary to adopt an iterative strategy, in which, the FE models for the vehicle and the supporting structure are developed in their uncoupled state and the dynamic interactions are studied *via* externally developed subroutines (Green and Cebon 1996). Such an uncoupled analysis is also deemed expedient to achieve computational efficiency in the treatment of VSI problems (Yang and Fonder 1996). In the context of the RPV-Launcher dynamic analysis, a schematic view of the modeling and the iterative solution strategy is shown in figure 5. Some of the important features of this scheme and some of the key assumptions made are as follows:

(a) The dynamics of RPV mounted on the shuttle and the launcher are considered separately.
(b) The forces of interactions between these two components are analyzed in an iterative manner. The entire analysis is carried out within the framework of linear vibration theory.
(c) The response of the RPV to the excitation caused by the track unevenness is studied first. During this analysis, the RPV is assumed to travel on rigid but uneven surface. The inputs are functions of not only the track unevenness, but also, they are dependent on the velocity and acceleration of the vehicle. The loads transmitted to the support through the wheels are recorded.
(d) The wheel loads from the preceding analysis are now applied on the launcher. These loads travel on the launcher with velocity v and acceleration a.
(e) The deflection of the launcher due to the passage of the wheel loads generates dynamic track unevenness for the RPV thus providing a feedback to the RPV.
(f) The response of the RPV to the launcher feedback is analyzed next. This, in turn, provides the improved estimates of the wheel loads on the launcher. This iteration cycle has to be repeated till the estimates of the wheel loads converge.
(g) The other sources of dynamic action on the launcher and the RPV are handled separately and the response contributions from individual sources of dynamic action are finally summed up.
(h) Each phase of the analysis is carried out using numerical integration of the uncoupled modal equations of motion for the RPV-shuttle model and the launcher model.

4.0 Dynamic wheel loads and the launcher feedback

As a first step in the analysis, FE models for the RPV-shuttle system and the launcher are made. The launcher is made up of steel while the RPV has parts made up of aluminum and fibre reinforced plastic (FRP). The FE models were constructed using discrete mass, 3D beam, shell and layered composite shell elements. Figure 6 illustrates the FE model for the RPV-shuttle system. This model has about 9200 dofs and the first few natural frequencies were found to be 3.58, 6.00, 6.85, 7.05 and 9.26 Hz. The RPV, when released form the shuttle, was found to have first few natural frequencies as 6.85, 7.10, 9.30, 9.86

and 12.62 Hz. These numbers were found to show good agreement with the corresponding experimental observations. Similarly, the first five launcher natural frequencies were found to be 8.31, 9.37, 14.48, 17.08 and 20.53 Hz. The total mass of the RPV-shuttle system was about 420.2 kg and that of the launcher was 2445.89 kg. It has been assumed that damping for the RPV and the launcher is modal viscous with 4% damping for all the modes. To determine the wheel loads due to guide way unevenness, the track unevenness on the launcher rails were measured. Figure 7 illustrates the track unevenness on one of the rails. As has been already mentioned, the launcher is fitted with six rails on which the shuttle wheels travel. In the present study, the unevenness profile of each of the six rails was measured separately and they were found to be dissimilar. The ensuing analysis takes into account this feature. If *R(x)* denotes the guideway unevenness, the acceleration at the wheel point, as the vehicle travels on the rails, is obtained as

$$\frac{D^2}{Dt^2}R[x(t)] = a\frac{\partial R}{\partial x} + v^2\frac{\partial^2 R}{\partial x^2} \quad ....(3)$$

where (*D/Dt*) stands for the total derivative and $x(t)=vt+0.5at^2$. The RPV response to the above acceleration was analyzed using direct integration methods. Figure 7 also shows one of the support acceleration for the case of exit velocity = 40 m/s. Here it is to be noted that RPV is in touch with the launcher at 12 points and each of these points suffer different support accelerations. The RPV response here can be handled by using the large mass concept as described for example in the book by Gerardin and Rixen (1997). Figure 8 shows the response at one of the bulkheads of the RPV due to ride on the uneven tracks. This calculation leads to the computation of the net wheel forces transferred to the launcher. The launcher response to the moving wheel loads was subsequently analyzed using the moving load option available on the NISA platform. If *Y(x,t)* is the deflection of the launcher rail, then the acceleration feedback to the RPV system is given by

$$\frac{D^2}{Dt^2}Y[x(t),t] = \frac{\partial^2 Y}{\partial t^2} + a\frac{\partial Y}{\partial x} + 2v\frac{\partial^2 Y}{\partial x \partial t} + v^2\frac{\partial^2 Y}{\partial t^2} \quad ....(4)$$

Figure 9 shows the RPV response due to the launcher feedback. The dynamic amplification of the wheel loads due to the RPV-shuttle ride on the uneven track for one of the wheels is shown in figure 10.

5.0 Other sources of excitation

The steps outlined in the previous section essentially characterize the RPV response to the effects of RPV motion, dynamic interactions between RPV and launcher and the guide way unevenness. As has been already mentioned, there exist several other sources of vibration, which also need to be handled concurrently. These effects are briefly described below:

1. **Transients due to rocket blast and shear pin break**: To initiate the motion of the shuttle-RPV system, the total thrust developed by the rockets must overcome the tensile strength of the shear pins and also the friction that exists between the

launcher rails and the shuttle wheels. Between the time of firing of the rockets and the time at which the RPV-shuttle system starts moving, it is assumed that the thrust developed by the rockets is transferred to the RPV shuttle as a vibration input. It must be noted that, while the tensile strength of the shear pins can easily be calculated, the estimation of the force required to overcome the friction is not easy. Based on the study of the high-speed photography records, it was observed that the shuttle starts moving after about 50 ms from the time of firing of the rockets. Figure 11 shows the details of the assumed variation of the total thrust developed by the rockets.

2. **Transients due to release of the aircraft from the shuttle arms**: Let $t=t^*$ be the time at which the aircraft separates from the shuttle. For $t<t^*$, the RPV remains mounted on the shuttle and its dynamics is governed by the vibration characteristics of the RPV-shuttle combine. However after $t=t^*$, the RPV dynamics is governed solely by the vibration characteristics of the airborne RPV. Thus, it follows that the system natural frequencies and mode shapes of the RPV undergo a transition at $t=t^*$. This sudden change in the configuration of the system would induce transient effects in the RPV.
3. **Engine induced response**: The power spectral density function of the force due to running engine was estimated using an inverse procedure using experimentally measured acceleration response at the engine base and analytically derived direct receptance at the engine mount location. Following this, a stationary random vibration analysis was carried out on the RPV-shuttle system to estimate the expected peak response of the RPV.
4. **Rocket exhaust effect**: To model this, it was assumed that 0.6 percent of the total rocket thrust gets converted into acoustic power and the PSD of this excitation is taken to be a space-time band limited white noise over a frequency range of 0-500 Hz. This enabled an estimate of the expected peak response of the RPV due to the rocket exhaust effect.

Table 1 summarizes the peak acceleration responses at a few crucial points on the RPV. The time history of acceleration response due to the combined action of various sources of excitations at the RPV nose is shown in figure 12. The trend of the response observed in this figure matched very well with field observations (see figure 3). The initial portions of the response here ($0<t<0.25$s) is mainly due to the combined action of transients due to shear pin break, rocket thrust and acoustic excitation due to rocket exhausts. Towards the end the vibration levels again build up due to pronounced RPV-launcher interactions. At the time of exit, there occurs a sharp spike in the response that is caused due to the “shake hand” effect caused during the release of the aircraft from the shuttle arms. In the field observations that were made (figure 3) the root mean square value of the acceleration was found to be about 18.6g at gimbal, 4.8g at equipment bay and 8.4g at nose. Furthermore, a peak response of about 50g was observed at all these locations near the time instant at which the aircraft gets released from the shuttle. The mathematical model qualitatively succeeds very well in explaining these observations.

6.0 Discussion and conclusions

A brief outline of the procedures followed in conducting dynamic interaction study on the RPV-launcher system has been provided in the preceding sections. Many details of the study could not be included in the discussion due to lack of space. Based on the matter presented in this paper, and, based on detailed investigations made during the study, the following conclusions are reached:

- The major contributions to response are made by excitations due to track unevenness, transient effects caused by the release of aircraft from the shuttle arms and the rocket exhaust impinging on the aircraft. The other sources of dynamic actions, namely, transients due to shear pin snapping, launcher feedback and engine induced excitations produce lesser levels of response.

- Notable difficulties are present in predicting the exact nature of the shuttle wheel and launcher rail contact scenarios. The present study has investigated several possible scenarios. We have obtained the peak response by taking it to be equal to the maximum of response predicted by assuming different wheel-rail contact scenarios.

- It was observed that the predictions based on FE analysis matched reasonably well with the field observations especially for the response near the nose and the first FRP bulkhead regions.

- Reduction in the exit velocity from 40 m/s to 36 m/s did not always guarantee reduction in response levels.

- The response due to track unevenness is pronounced towards the end of launching when the RPV-shuttle combine travel at higher velocities. On account of the increased velocities towards the end, even small irregularities in these portions of the rail can induce significant dynamic response. Mechanisms responsible for production of track irregularities, especially in the portions of the rails at the end of launcher, needs to be understood. Maintenance of rail portions in this region is needed.

In closure, it may be remarked that FE modeling and analysis, as developed in this study, are valuable in ascertaining relative magnitudes of contributions to the total dynamic response due to diverse sources of excitations in a problem as complex as the RPV-launcher dynamics studied in this paper.

7.0 References

1. Filho F.V. (1978) *Finite element analysis of structures subjected to moving loads*, Shock and Vibration Digest, 10(8), 27-35.
2. Fryba L. (1999) *Vibration of solids and structures under moving loads*, Thomas Telford Publishing House, Prague.

3. Fryba L. (1996) *Dynamics of railway bridges*, Thomas Telford, UK.
4. Genin J. and Ting E.C. (1979) *Vehicle-guideway interaction problem*, Shock and Vibration Digest, 11(12), 3-9.
5. Geradin M. and Rixen D., (1997), *Mechanical vibrations: theory and application to structural dynamics,* John Wiley, Chichester.
6. Green M.F. and Cebon D. (1996) *Dynamic interaction between heavy vehicles and highway bridges*, Computers and Structures, 62(2), 253-264.
7. Kirkegaard P.H., Nielsen, S.R.K. and Enevoldsen I. (1997) *Heavy vehicles on minor highway bridges – a literature review*, Structural Reliability Theory Paper No. 169, Department of Building Technology and Structural Engineering, Aalborg University, Denmark.
8. Lin Y.H. and Tretheway M.W. (1990) Finite *element analysis of elastic beams subjected to moving dynamic loads*, Journal of Sound and Vibration, 136(2), 323-342.
9. Ting E.C., Genin J. and Gunsberg J.H. (1975) *Dynamic interaction of bridge structure and vehicles*, Shock and Vibration Digest, 61-69.
10. Yang F. and Fonder G.A. (1996) An *iterative solution method for dynamic response of bridge-vehicle systems*, Earthquake Engineering and Structural Dynamics, 25, 195-215.

Figure 1 The RPV and launcher system

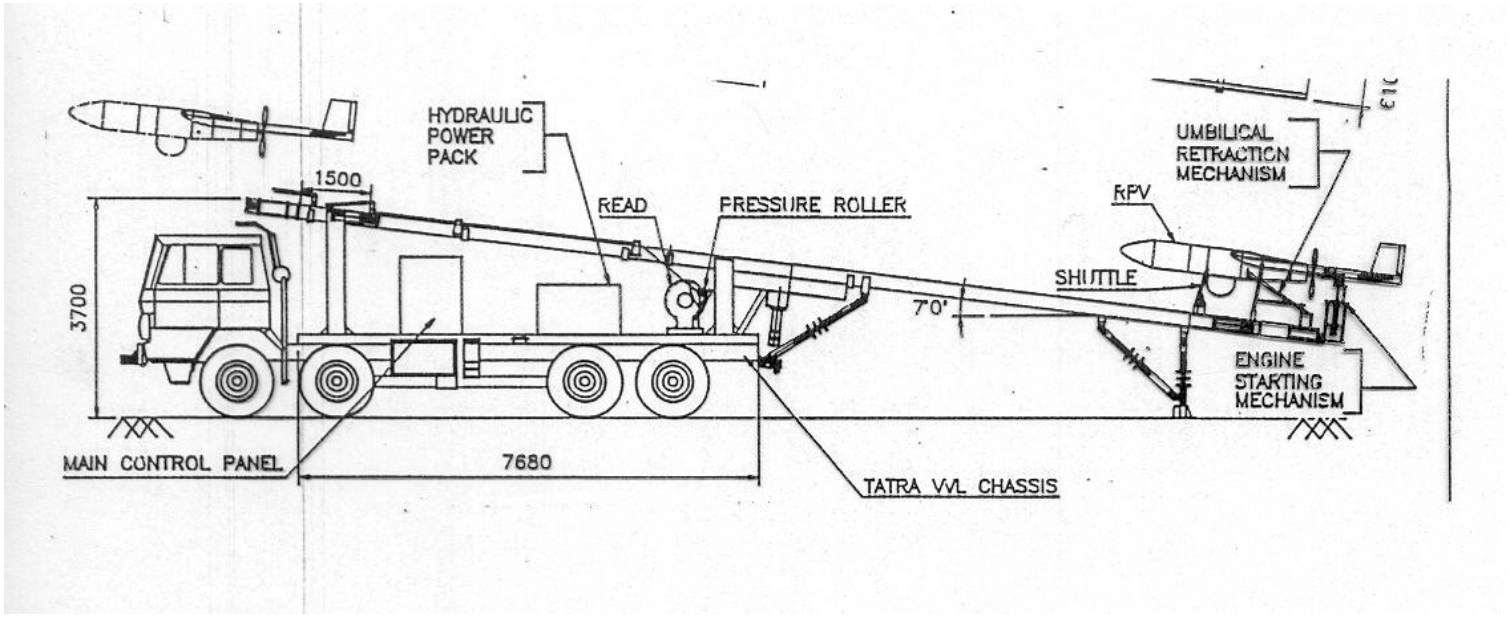

Figure 2 Parts of the RPV-launcher system

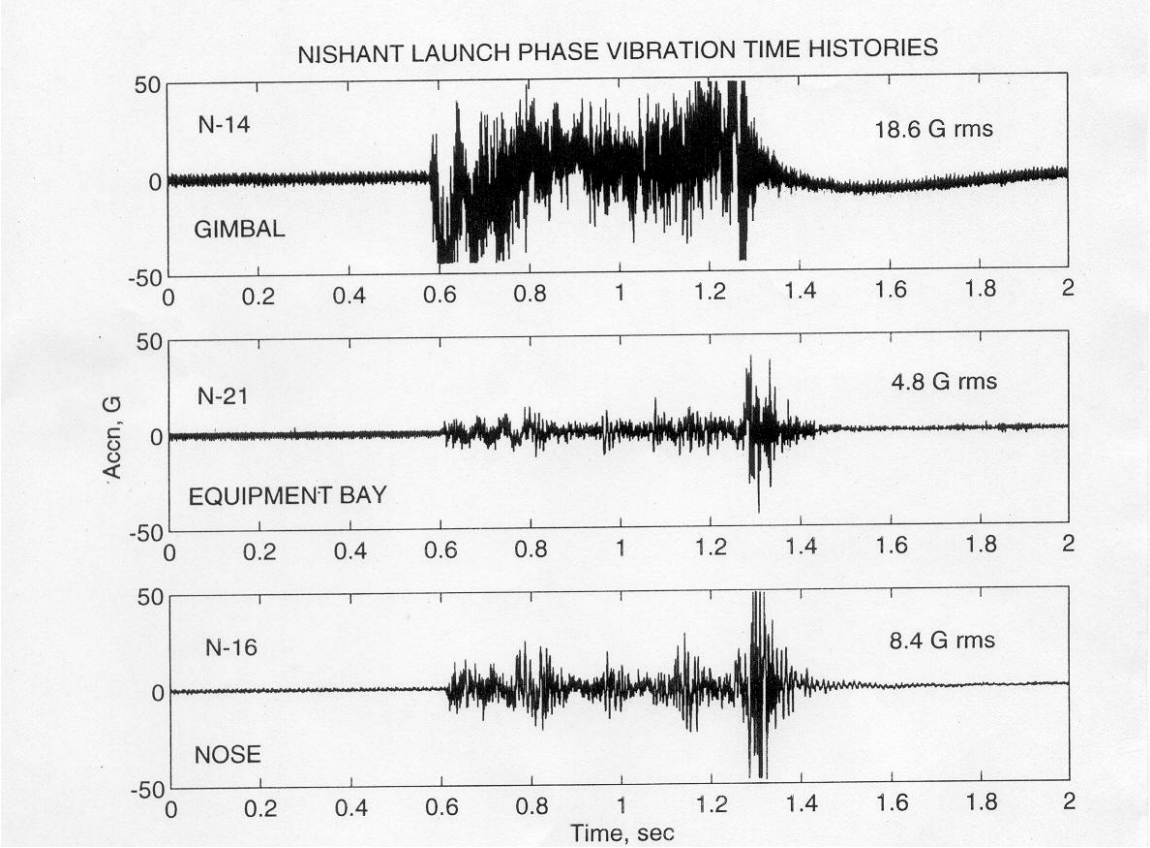

Figure 3 RPV response measured in the field

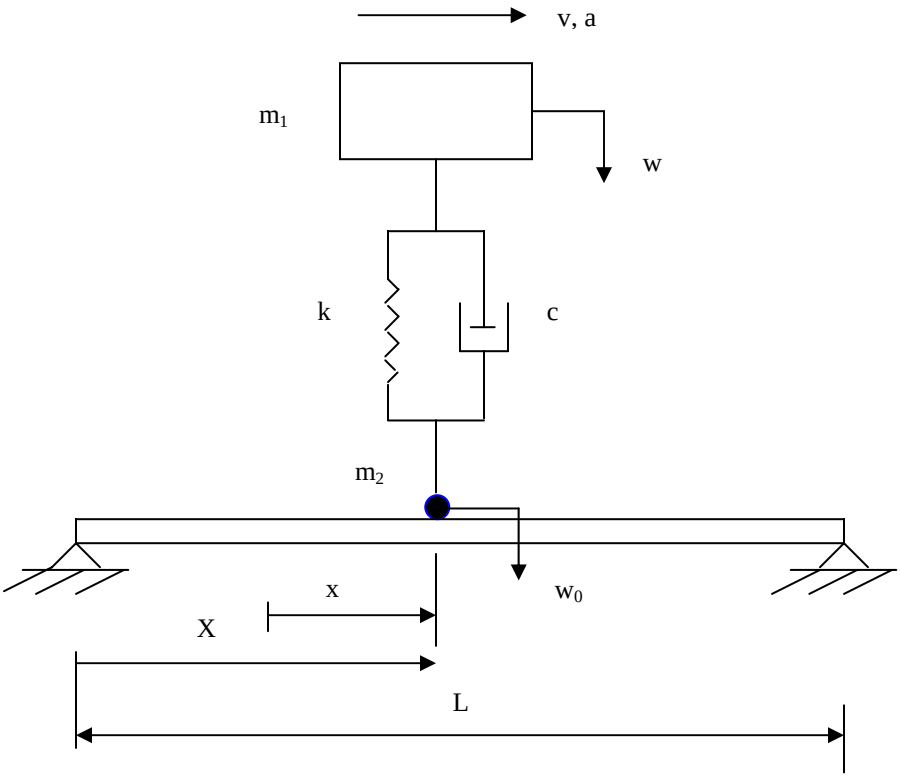

Figure 4 A beam and moving oscillator system

Figure 5 Schematic of the RPV-Launcher dynamic response analysis

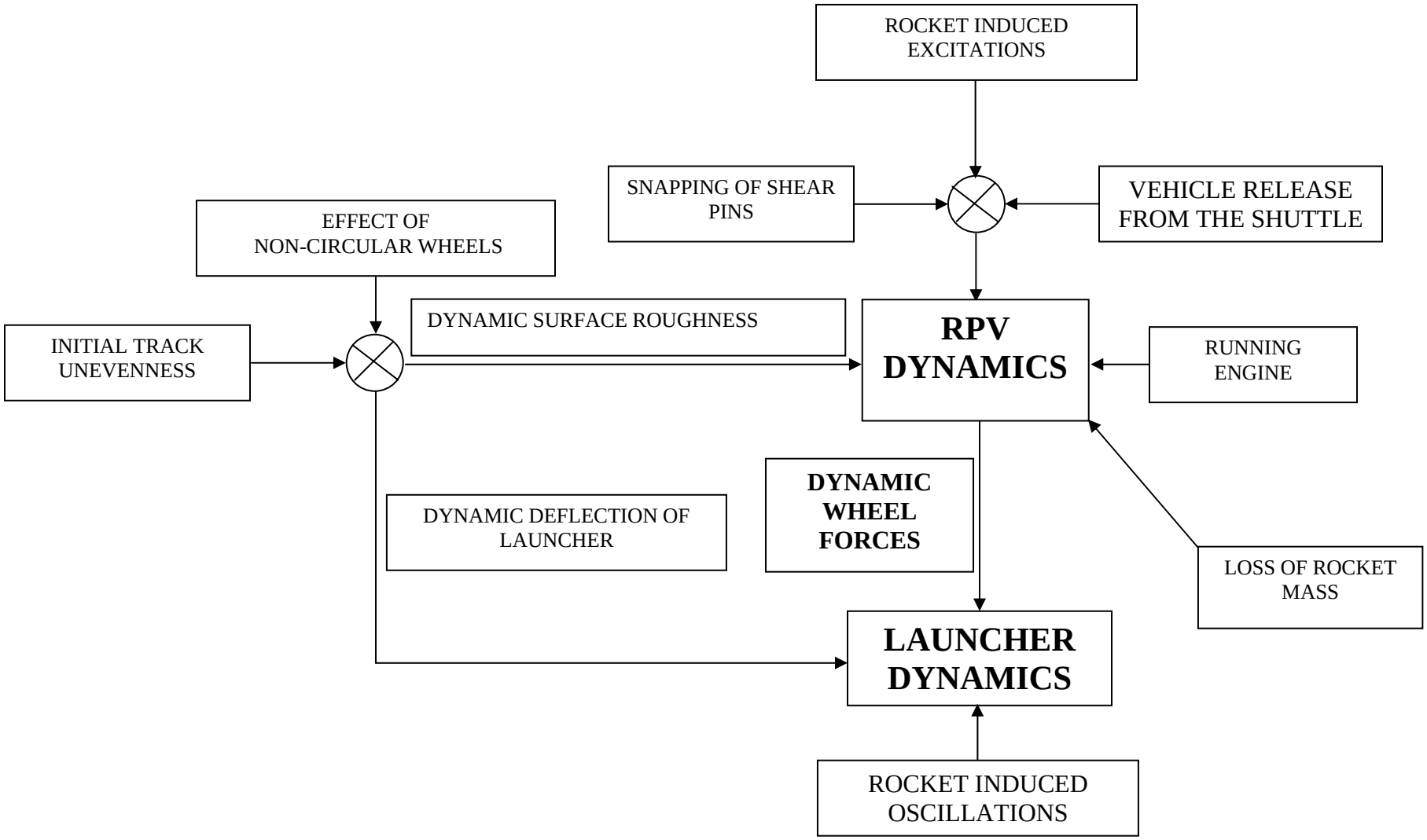

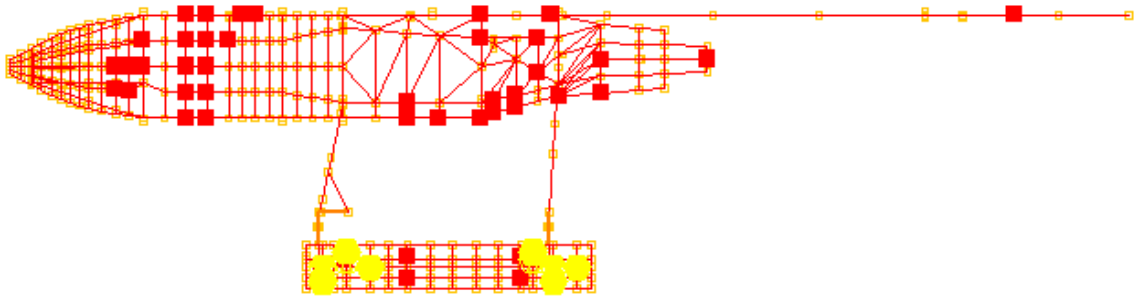

Figure 6 Model for the aircraft mounted on the shuttle

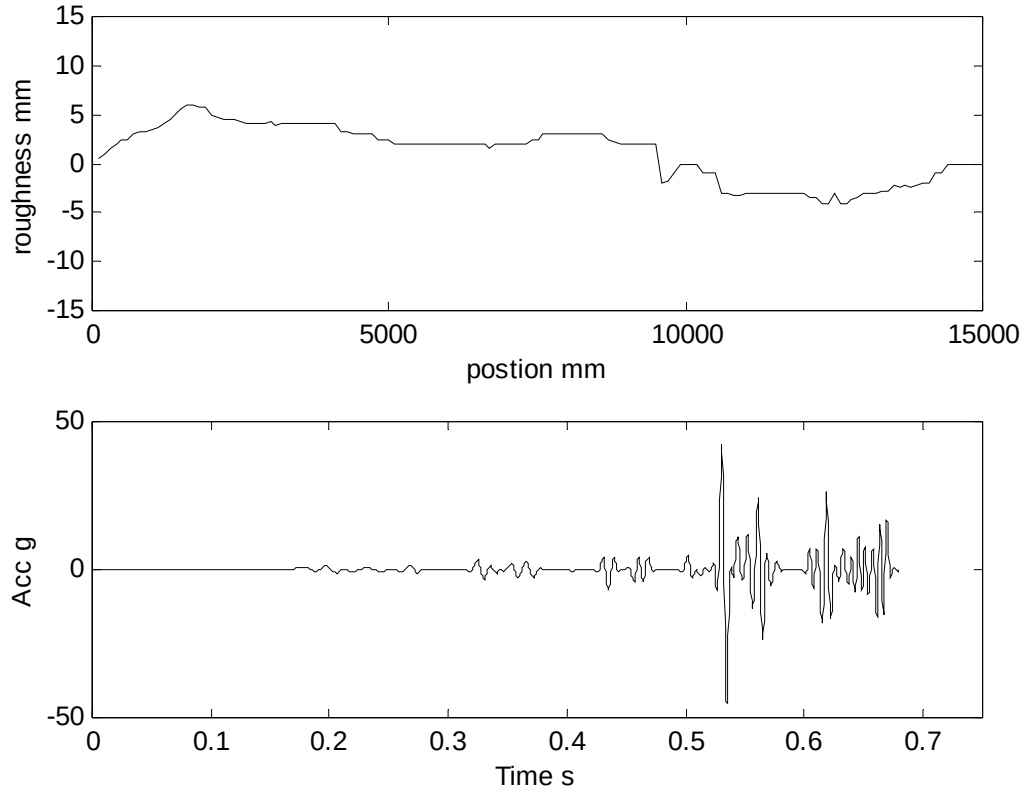

Figure 7 The measured track unevenness profile (top); the support accelerations due to track unevenness to be applied at the wheel points (bottom); exit velocity = 40 m/s for port side top rail.

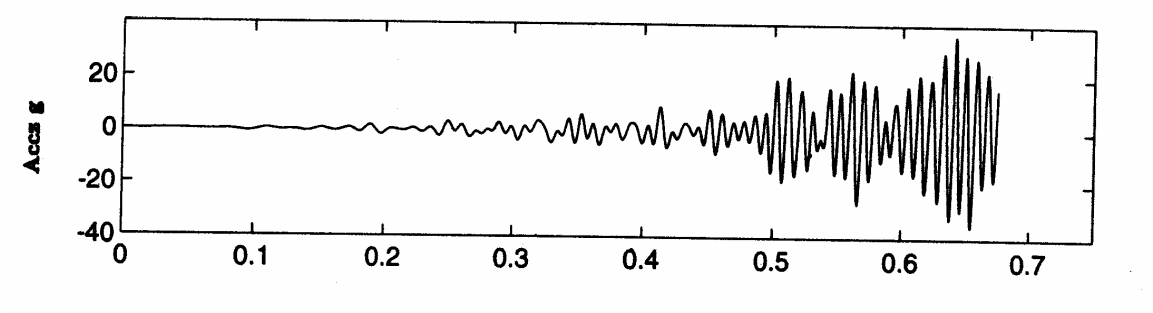

Figure 8 RPV response due to ride on uneven tracks; exit velocity = 40 m/s (FRP bulkhead).

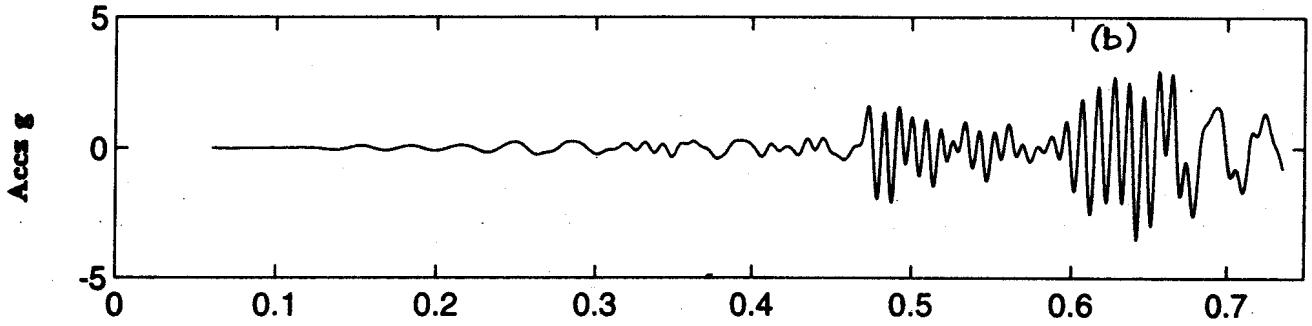

Figure 9 RPV response due to launcher feedback; FRP bulkhead

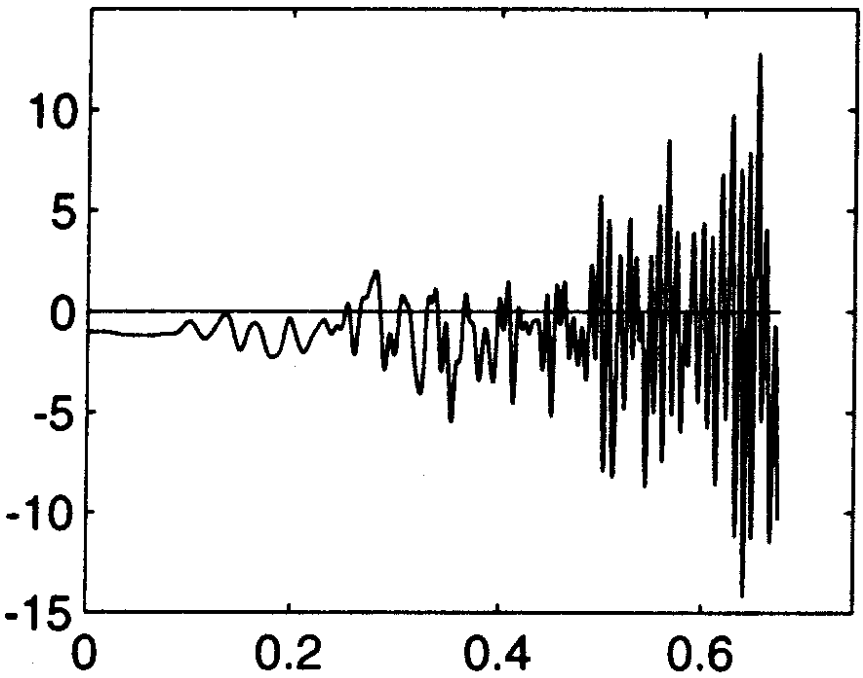

Figure 10 Dynamic magnification of the wheel loads due to RPV-shuttle ride on uneven track ; Port side front wheel

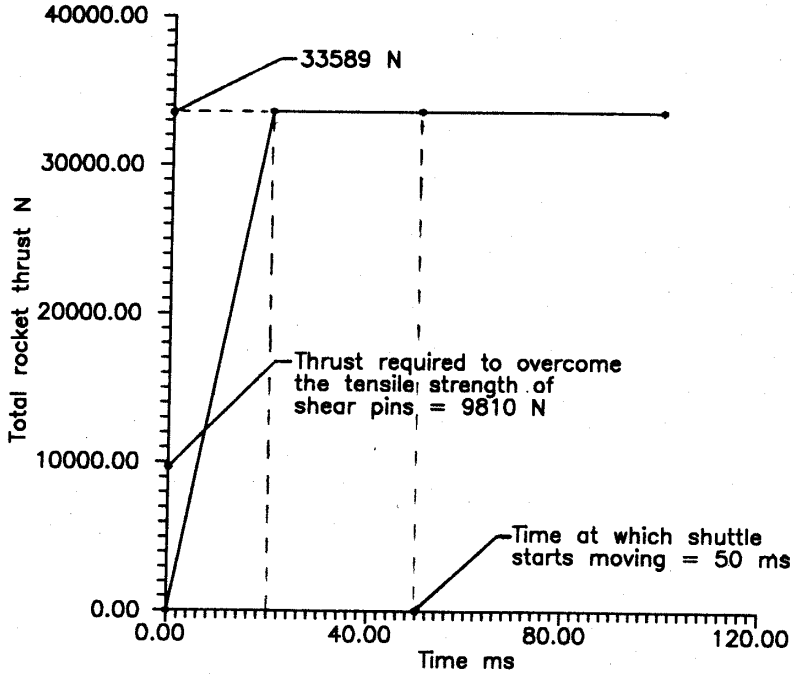

Figure 11 The total thrust developed by the rockets

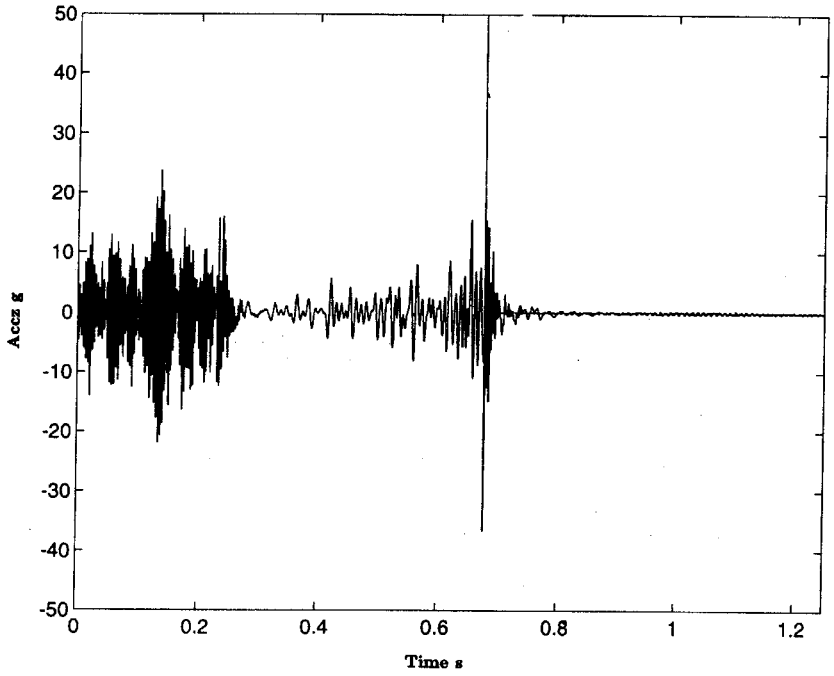

Figure 12 Cumulative response due to the action of various sources of excitations at the RPV nose.

Table 1: Summary of peak acceleration responses in z-direction due to different sources of dynamic action.

Source of dynamic action	Nose	First FRP Bulkhead	First Metal Bulkhead
Track unevenness	39.2 g	36.3 g	21.4 g
Launcher feedback	2.5 g	3.5 g	2.2 g
Initial transients including snapping of shear pins	1.7 g	0.2 g	2.3 g
Release of aircraft from shuttle	30.0 g	17.6 g	52.0 g
Engine (up to 500 Hz)	2.3 g	1.2 g	0.4 g
Rocket exhaust	5.3 g	0.8 g	23.8 g